

# LASER-STIMULATED DESORPTION FROM $\text{CaF}_2$ CRYSTALS

E. MATTHIAS, S. GOGOLL, E. STENZEL and M. REICHLING

*Fachbereich Physik, Freie Universität Berlin, Arnimallee 14, 14195 Berlin, Germany*

*(Received May 30, 1993)*

Optical transmission and laser-induced desorption (LID) of neutral particles and positive ions from optical-grade  $\text{CaF}_2$  has been studied, using nanosecond laser pulses of 532 nm. Two different emission characteristics were found: one for which the breakdown of transmission coincides with the onset of ablation; and another for which the transmission breakdown occurs at about 20–30% lower fluences compared to the ablation threshold. In the latter case the transmission breakdown is accompanied by delayed (tenths of seconds) particle emission. We propose that the particle emission below the ablation threshold is defect-assisted LID, in the sense that light absorption by preexisting defects leads to local heating and thermal expansion, causing microcracks from which particles are ejected.

*Keywords:* fluorite, laser-induced desorption, ablation threshold, optical transmission, XPS.

## 1 INTRODUCTION

In contrast to massive material removal above the ablation threshold, laser-induced desorption (LID) should be defined as emission of individual particles under the influence of pulsed laser light *below* the ablation or damage threshold fluence. The main area of LID in the past was the desorption of adsorbates from well-defined surfaces under the influence of light. This type of work is not addressed here, and the interested reader is referred to a review of the subject by Chuang<sup>1</sup> and other relevant papers, for example Refs. 2,3. In our project we are concerned with the desorption of individual particles from polished or cleaved surfaces of ionic crystals when these are irradiated in UHV with nanosecond laser pulses of sub-bandgap photon energies.<sup>4</sup> The motivation is twofold: (1) We suspect that LID is the precursor of optical damage and we want to find out under which conditions it occurs. (2) We ask the question to what extent there are similarities between electron- and laser-stimulated desorption.

The literature on LID from clean surfaces of wide bandgap crystals is not overly abundant. Much of the time-of-flight mass spectrometry or laser-induced fluorescence work does not qualify in this category since it was carried out at higher fluences and the state of the surface was of little concern. One of the earliest reports on LID was by Schmid *et al.*<sup>5</sup> about the directional emission of halogen atoms from KBr and KCl crystals along the  $\langle 110 \rangle$  and  $\langle 211 \rangle$  directions, indicating that H-centers would move to the surface by means of a focussed collision sequence. The authors also showed that the excitation process was a 4-photon absorption of ruby laser light. These observations suggested that—apart from the excitation mechanism—the mechanism for LID is similar to the one for electron stimulated desorption (ESD).

Other reports were by Chase and Smith<sup>6</sup> on  $\text{Na}^0$  emission from NaF at about half the damage threshold fluence for 266 nm light, or by Arlinghaus *et al.*<sup>7</sup> on  $\text{Zn}^0$  emission from ZnS at about one third the damage fluence at 308 nm. Multiphoton photoemission from CdTe, ZnS, and NaCl was observed by Siekhaus *et al.*,<sup>8</sup> and by Matthias *et al.*<sup>9</sup> from  $\text{BaF}_2$ . Also reported in Ref. 9 was a wavelength and polarization dependent emission of positive ions, among others  $\text{F}^+$ , proposed to originate from multiphoton absorption of pulsed laser

light in the green spectral range.<sup>10</sup> There are more papers on the subject in the literature (see for example Refs. 11–21), still there is no detailed understanding of all processes involved and subthreshold desorption rates at a given wavelength cannot be predicted for any wide bandgap material. On the other hand, a few facts are established like, e.g., defect states in the band gap promote photon absorption,<sup>4,11,17</sup> laser-induced electronic defects play a role in the desorption mechanism,<sup>5,16,18</sup> and fracture significantly contributes to particle emission.<sup>20</sup>

The general tendency is to assume that in LID multiphoton absorption leads to the production of self-trapped excitons and subsequently, with a certain efficiency, to separated F-H pairs.<sup>5,16,22,23</sup> The accumulation of color centers at subthreshold fluences is called 'incubation',<sup>4,24</sup> and is held responsible for multishot damage observed in crystals or optical coatings. The energy transport to the surface and the desorption dynamics is thought to proceed similarly to the steps observed in ESD.<sup>5,16,18</sup> However, to our knowledge there are no reports yet where both techniques have been applied under identical conditions to the same type of crystal with the goal of comparing the mechanisms involved in LID and ESD. Toward this objective we have started a project with CaF<sub>2</sub>, and elected this crystal because much is known about its color centers.<sup>25,26</sup> However, we are not aware of any ESD results on CaF<sub>2</sub>.

## 2 EXPERIMENTAL TECHNIQUES

To unravel the complexity of desorption dynamics, complete experiments should be carried out on well-defined surfaces, measuring as many quantities as possible. For this purpose the measurements must be carried out in a UHV chamber, equipped with some analytical tools to characterize the surface. The experimental set up used for our measurements is sketched in Figure 1. The final goal is to observe the optical properties of the surface and the change of its stoichiometry during laser irradiation simultaneously with the emission of ions, neutrals, and electrons. As a light source we used a Quanta-Ray DCR-3 Q-switched Nd:YAG laser, equipped with injection seeder and harmonic generator. In future it is planned to also install a dye laser and to examine the dependence of LID on wavelength and pulselength.

In this paper we present mass spectroscopic data on Ca<sup>10</sup>, F<sup>19</sup>, CaF<sup>40</sup>, and F<sup>+</sup> as a function of laser fluence. The emission was stimulated by 7 ns laser pulses at 532 nm wavelength in an N-on-1 irradiation mode. In addition, the optical transmission of the crystal was

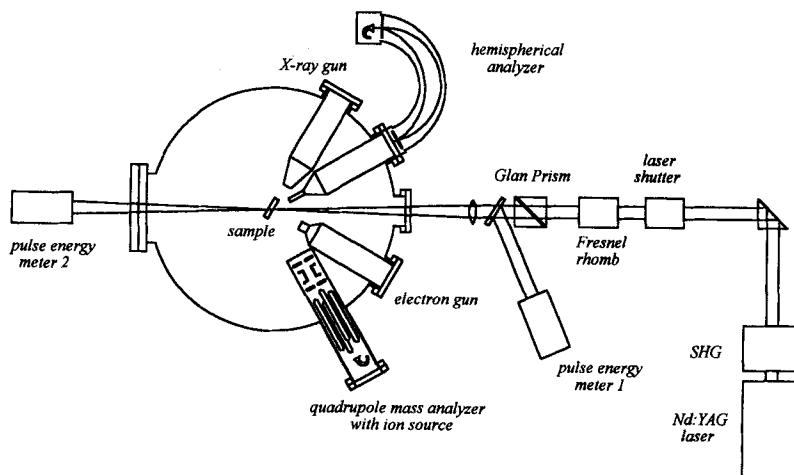


FIGURE 1 Principle scheme of the experimental set up.

monitored during the measurements. The laser beam profile was donut-shaped, and the focus at the crystal surface had a diameter of approximately 0.2 mm. A few hot spots in the beam profile could cause some uncertainty in the power density quoted in the figures. The fluence was varied by means of a Fresnel rhomb in combination with a Glan prism (see Figure 1). Typically, a run started at low fluences where no emission was recorded and where the crystal was fully transparent. Then the fluence was stepwise increased for each laser shot. Note that this procedure involves two effects: the accumulation of defects during the N-on-1 irradiation, and the influence of an increasing pulse energy on LID.

The experiments were carried out on optically polished UV-grade single crystals of  $\text{CaF}_2$  from Dr. Karl Korth oHG, Kiel. The only additional surface preparation consisted of heating the crystals up to  $350^\circ\text{C}$  for several hours in order to force desorption of weakly bound contaminants. Polishing scratches of typically a few nanometer depth remained as predominant structural surface defects. As shown in Figure 2, XPS analysis revealed that carbon and oxygen were the most abundant impurities in the surface layer.

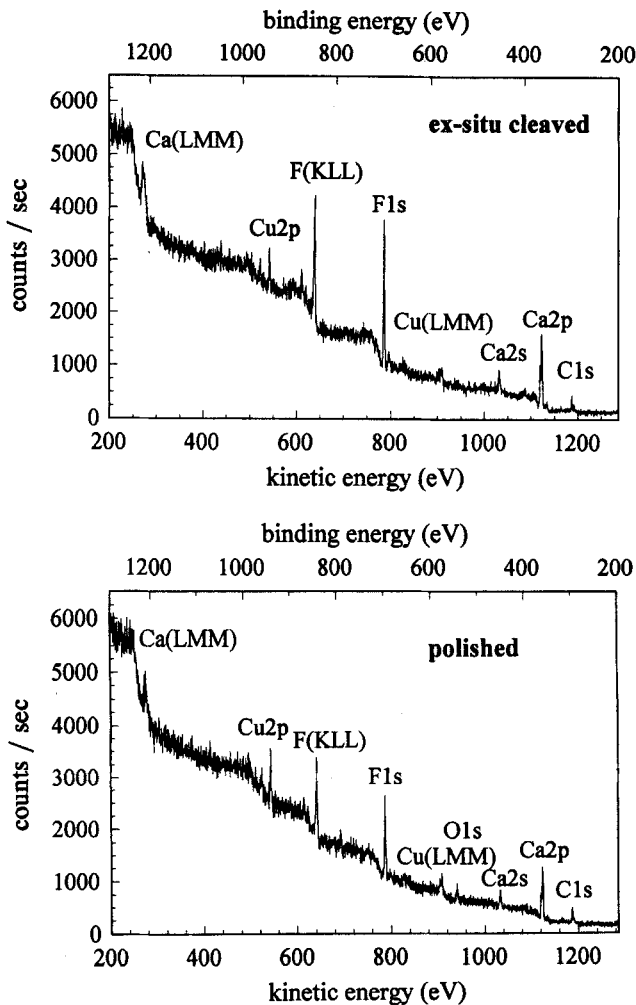


FIGURE 2 XPS spectra (Al anode source) of cleaved (upper part) and polished (lower part)  $\text{CaF}_2(111)$  surfaces, before heating the crystals.

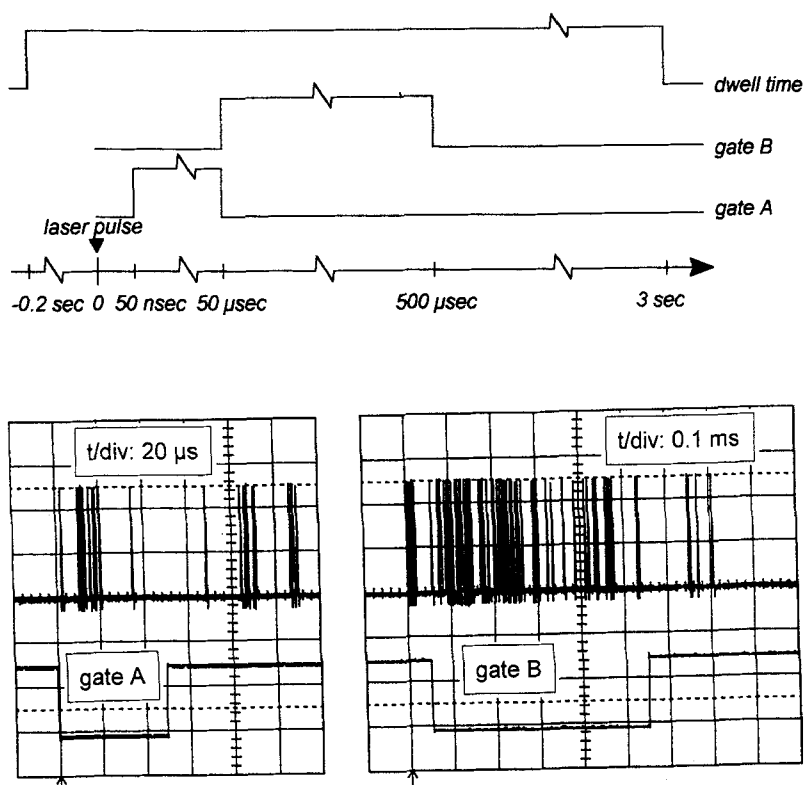


FIGURE 3 Gate settings for the mass analyzer (upper part). The lower part shows a typical time distribution of mass selected  $\text{CaF}^{(0)}$  signals in gate B. In gate A appears a group of fast ions which due to their speed escaped mass selection.

The emitted particles were registered by a quadrupole mass spectrometer, furnished with an ionization device for detecting neutrals. To estimate kinetic energies of ions or to suppress unwanted ion signals, the entrance grid of the mass filter could be charged to +100 V with respect to the sample holder. This repulsion potential was on for all desorption measurements of  $\text{Ca}^{(0)}$ , it was switched off, however, when positive ions (like  $\text{F}^+$ ) were detected. At the highest laser intensities a signal was observed even when the ionization current was switched off. This was attributed to the emission of ions from the laser-induced plasma with kinetic energies exceeding 100 eV. The distance between crystal surface and ionization area of the mass filter was approximately 40 mm, introducing a flight time that allowed a coarse grouping of the particles with regard to their arrival time at the detector. We distinguish between fast (nonthermal), slow (essentially thermal), and delayed particles. To obtain the fluence dependence of the yield for each group, the output pulses of the mass analyzer were collected in three different time intervals: gate A: 50 ns to 50  $\mu\text{s}$ , gate B: 50  $\mu\text{s}$  to 500  $\mu\text{s}$ , and a total acceptance time from -0.2 s to 3.0 s. The gate setting is indicated in the upper part of Figure 3. A typical signal distribution in the time range of the first two gates is illustrated in the lower part of Figure 3, with the mass analyzer set to  $\text{CaF}^{(0)}$ . The arrows indicate time zero when the laser fired. In both gate settings, one recognizes a fast signal group appearing during the first 20  $\mu\text{s}$ . Most likely, these are ions which, due to their speed, are not mass analyzed. The signals in gate B represent mass-selected neutral  $\text{CaF}^{(0)}$ . A few signals outside gate B indicate that there is delayed emission, which for  $\text{Ca}^{(0)}$  extends up to tenths of seconds.

### 3 RESULTS AND DISCUSSION

#### 3.1 XPS Results

Photoemission techniques will be employed to monitor the stoichiometry of the surface before, during and after laser or electron irradiation. The low flux of photoelectrons avoids charging, and the mean free path of the electrons ensures sensitivity to a shallow depth near the surface. In Figure 2, XPS spectra taken from a cleaved (upper frame) and a polished (lower frame)  $\text{CaF}_2(111)$  surface are displayed. The spectra were taken before heat treating the crystals. Two features are apparent: (1) there is some contamination of C and O; (2) the relative abundance of Ca and F differs in both cases by about 25%. This latter observation deserves attention. If we assume that the polishing procedure does not significantly change the stoichiometry of the probed near-surface volume, it means that the *crystals age by bleeding out neutral fluorine*. This agrees with the familiar observation that fluorites always cause a background pressure of fluorine in the UHV-chamber. To our knowledge the mechanism for such 'spontaneous' desorption of  $\text{F}^{(0)}$  is not understood, although we suspect that laboratory light may play a role in activating the process. The important consequence is that the crystals will, with time, develop defect centers which, in turn, can serve as absorption centers for light. Hence for 'aged' crystals one would expect a higher desorption rate at a given fluence and a lower damage threshold compared to freshly cleaved crystals. We have not been able to observe such behavior, the reason may be that cleaving always causes structural defects on the surface. The difference in stoichiometry between freshly cleaved and aged polished crystals vanishes when annealing them for several hours at  $400^\circ\text{C}$ .

#### 3.2 Optical Transmission

As indicated in Figure 1, the transmission of the laser beams is monitored during all measurements. This yields information about the decline of optical properties of the crystals which, after all, should be perfectly transparent to 532 nm radiation. In general, loss of transmission can occur by scattering and/or absorption. In the crystal bulk, absorption could be caused by color centers and scattering by colloids and structural defects. At the surface, structural damage would give rise to scattering. We tend to believe that scattering at the surface is the main reason for transmission loss.

The dependence of transmission on fluence for multishot irradiation (N-on-1 mode) can be seen in Figure 4, together with data on particle emission. We reproducibly observe *two types of spots* with distinctly different transmission behavior that goes along with a different emission characteristics. The general trend is that the transmission sharply drops at a certain fluence. This breakdown is rather abrupt when it coincides with the ablation threshold, as shown in the lower part of Figure 4. We propose that such pattern is typical for a *'clean' surface spot with low defect density*. In this case the ablation threshold fluence is high and when it is reached, the sudden surface damage caused by dielectric breakdown<sup>27</sup> leads to strong scattering and a steep drop in transmission. This interpretation is supported by the smooth and constant transmission data below the breakdown threshold.

In contrast, the data in the upper part of Figure 4 show a much less abrupt decrease of transmission about 30% below the ablation threshold. This type of spot is found to occur about 2.5 times more abundant than the one in the lower picture of Figure 4. Also, during transmission breakdown neutral calcium is emitted which becomes dormant again at further increasing fluences. Both points are corroborated by another set of data shown in Figure 5. We believe that this behavior is characteristic for a *spot with large defect density*, however, the detailed mechanism is not understood. In general, there are two possibilities: one is color center production in the bulk and transmission breakdown by absorption, the other

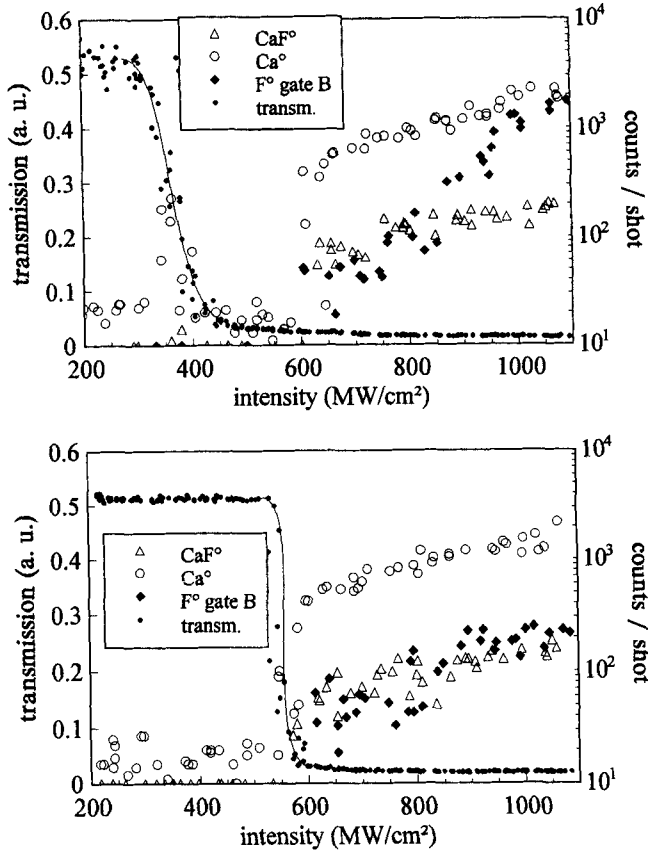


FIGURE 4 Optical transmission and particle emission from  $\text{CaF}_2(111)$  surfaces as a function of fluence at 532 nm for two different spots (upper and lower frame). The data were recorded at room temperature with a total of 200 laser shots on one spot (N-on-1 irradiation mode). The gate setting was 3.0s for  $\text{Ca}^{(0)}$  and  $\text{CaF}^{(0)}$ , while  $\text{F}^{(0)}$  was registered in gate B only.

is development of microcracks at or near the surface and transmission loss by scattering. We favor the latter, realizing that it upsets the commonly held view that thermal effects are no major issue whenever the photon energy is much smaller than the band gap.<sup>16</sup> Further investigations, for example, detection of light scattering and in situ measurements of the stoichiometry will be necessary to elucidate this problem.

### 3.3 Desorption of Neutrals

In Figure 4, the emission of  $\text{Ca}^{(0)}$ ,  $\text{CaF}^{(0)}$ , and  $\text{F}^{(0)}$  during a time interval of 3.0 s after the laser pulse is shown as a function of fluence for multishot irradiation of one spot. As discussed above, on spots with low defect density (lower part of Figure 4) particle emission sets in suddenly at the damage or ablation threshold by dielectric breakdown and plasma formation.<sup>27</sup> In this fluence regime the emission of neutrals will also be accompanied by charged particle emission with high kinetic energies. Such group of fast particles can, for example, be recognized in the signal distributions displayed in the lower part of Figure 3. This behavior does not qualify as LID and will not be further discussed here. The reader is referred to the literature on ablation<sup>12</sup> and the review by Jones *et al.*<sup>23</sup> on optical damage in wide band gap crystals.

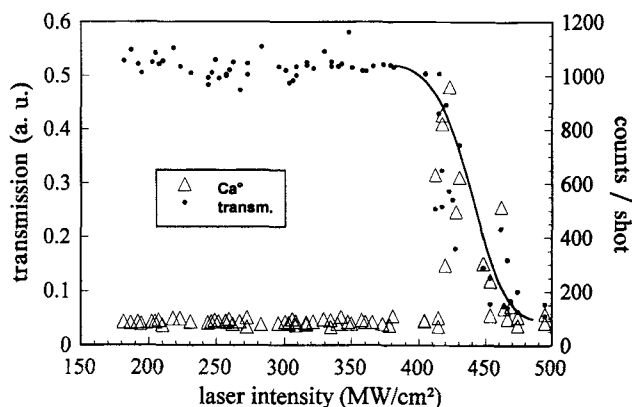


FIGURE 5 Dependence of optical transmission (dots) and LID emission of  $\text{Ca}^{(0)}$  (triangles) from  $\text{CaF}_2(111)$  on laser fluence at 532 nm. The data were taken in an N-on-1 mode on a spot that showed the two-threshold behavior displayed in the upper part of Figure 4. The measurement was carried out at room temperature; the accumulation time for  $\text{Ca}^{(0)}$  was 3.0s.

The upper frame of Figure 4 shows data for a spot with two thresholds. One where massive material ablation sets in at a somewhat higher fluence compared to the one in the lower picture. The other at about 30% smaller fluence, where the optical transmission breaks down and  $\text{Ca}^{(0)}$  is emitted. Another example of the neutral calcium emission at the transmission breakdown fluence is shown in Figure 5. We define this emission as genuine LID. For photon energies much smaller than the band gap it is assisted by defect states in the band gap.<sup>4,8,11</sup> Therefore, LID occurs only on those crystal areas where the defect density is sufficiently large. Light absorption can take place either by single photon excitation from occupied defect states in the band gap or by multiphoton absorption resonantly enhanced by unoccupied defect states in the band gap.<sup>4,11</sup>

Emission data like the ones in Figure 4 carry no direct information regarding the nature of the defects. In principle, the light absorbing centers can be impurities, color centers, or structural defects. However, in view of the results presented in Figure 4 and the relative abundance of 1:2.5 of 'clean' and 'defect-ridden' spots, we suggest that structural defects at or near the surface play the dominant role. It is unlikely that impurities and intrinsic defects are inhomogeneously distributed in the bulk of the crystal to cause such two-spot effect. Further support of this view comes from the fact that above the transmission breakdown the particle emission decreases again with increasing fluence and then remains dormant up to the ablation threshold. This observation would be hard to understand in connection with color centers, since an increasing fluence should produce more color centers and consequently an increase of the desorption rate.

It is more likely that the Ca emission originates from microcracks<sup>20,21</sup> which are caused by thermal stress following heating by photon absorption at structural defects at or near the surface. Once those microcracks are formed, the light is strongly scattered, thereby reducing further absorption and growth of the microcracks, and  $\text{Ca}^{(0)}$  emission ceases as soon as the existing cracks are metal depleted. Figure 6 presents more evidence for the conjecture that reduction of light absorption by scattering stops further particle desorption. It shows the transmission breakdown coincident with  $\text{Ca}^{(0)}$  emission as a function of successive laser shots. Again we notice that there is strong LID of  $\text{Ca}^{(0)}$  while the optical transmission decreases. However, as soon as the transmission is reduced by about 90%, the  $\text{Ca}^{(0)}$  emission drops to a value close to the noise and does not reactivate for the next 80 shots. To substantiate this model even further, it is necessary in future to also monitor the light scattered from the surface.

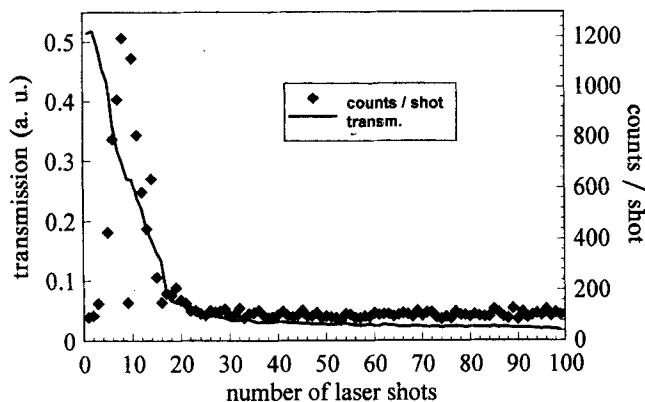


FIGURE 6 Optical transmission and LID of  $\text{Ca}^{(II)}$  from  $\text{CaF}_2(111)$  for successive laser shots (532 nm) on the same spot. The data were taken at room temperature; the accumulation time for  $\text{Ca}^{(II)}$  was 3.0 s; the laser intensity was approximately  $400 \text{ MW/cm}^2$ .

### 3.4 Delayed emission of $\text{Ca}^{(II)}$

Unexpected was the observation that the  $\text{Ca}^{(II)}$  emission for fluences around the transmission breakdown, as shown in Figures 4 (upper frame) and 5, is delayed by tenths of seconds and cannot, for example, be registered in gates A and B (cf. Figure 3). In Figure 7, a typical time decay of the desorption rate, averaged over the transmission breakdown range, in this case 20 lasershots, is shown. The measurement was carried out at room temperature. The fit of a single exponential function to the data yields a half-life of about 130 ms. The reason for this delay is still unknown and more data are needed to answer this question. If we accept the model of  $\text{Ca}^{(II)}$  originating from microcracks caused by thermal stress, we have the option to either identify the delay with the growth time of the cracks or to introduce a migration velocity of metal atoms along and out of those cracks. Further research on this point should aim to distinguish between these two alternatives.

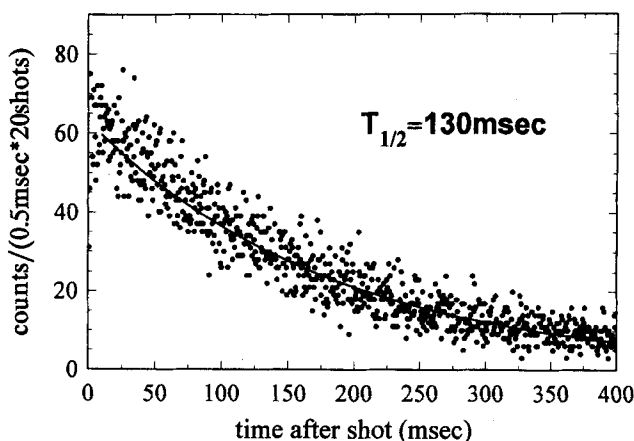


FIGURE 7 Time dependence of the delayed emission of  $\text{Ca}^{(II)}$  from  $\text{CaF}_2(111)$ , measured at room temperature. The data represent an average of the emission events at fluences around the transmission breakdown (cf. Figures 4 and 5), corresponding to 20 lasershots.

### 3.5 Desorption of $\text{F}^+$

Previous investigations of fluorites reported the observation of positive fluorine ions.<sup>9,19,28</sup> However, despite experimental evidence it was considered unlikely that  $\text{F}^+$  could be emitted from the crystal. Instead, gas phase ionization was suggested.<sup>29</sup> Also theoretical simulations came out against the emission of positive halogens from  $\text{NaF}$ <sup>30</sup> and  $\text{CaF}_2$ .<sup>31</sup> For this reason we measured  $\text{F}^+$  emitted from  $\text{CaF}_2(111)$  in all three time gates, with no positive potential between crystal holder and entrance grid of the quadrupole mass analyzer. The fluence dependence of the  $\text{F}^+$  signals together with the transmission results are displayed in Figure 8. The

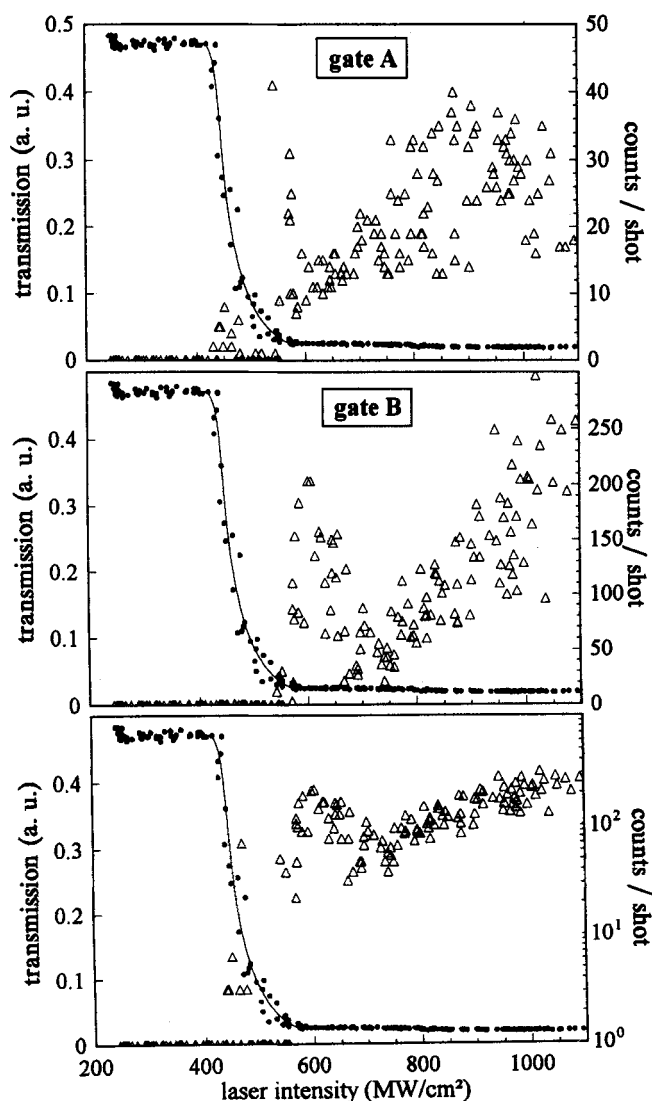


FIGURE 8  $\text{F}^+$  emission (triangles) and optical transmission (dots) of  $\text{CaF}_2(111)$  as a function of laser fluence at a wavelength of 532 nm. The measurement was performed in an N-on-I irradiation mode with the crystal at room temperature. The lowest frame shows the emission yield integrated over the full time interval of 3.0 s.

pattern identifies this spot as one showing the two-threshold behavior, where in this case the interval between the thresholds is somewhat smaller than, e.g., in the upper part of Figure 4. The obvious feature in Figure 8 is that the  $F^+$  emission peaks at the ablation onset, then reduces somewhat to increase again at high fluences where the plasma becomes optically dense. The flare up at the ablation threshold is curious but undoubtedly connected with the dielectric breakdown mechanism, and therefore not of interest in this connection. We do notice, however, a weak  $F^+$  emission right at the onset of the transmission breakdown in gate A and during the full dwell time of the mass analyzer (lowest frame). This emission must be attributed to defect-assisted LID. Gas phase ionization can be ruled out by lack of ionizing particles. One might speculate that the positive charge originates from charging inside the microcracks,<sup>32</sup> which would be consistent with the above proposed mechanism for LID of  $Ca^{(0)}$ .

#### 4 SUMMARY AND OUTLOOK

In this contribution, results for XPS, optical transmission and LID measurements on  $CaF_2$  single crystals are presented. One observation which needs to be investigated in more detail is the ‘aging’ effect of polished crystals, i.e. the fact that older crystals are fluorine depleted. Judging from the penetration depth of the photoelectrons it is unlikely that this effect can be blamed on the polishing procedure.

Another observation is the appearance of two types of spots on these commercial crystals with vastly different transmission and particle emission characteristics under irradiation with 532 nm light pulses. For one type of spots the optical transmission breakdown coincides with the onset of massive material ablation. We consider this to be the response of a crystal part with low defect density, for which the fluence can be increased until the dielectric breakdown limit. The other type of spots exhibits two fluence thresholds, one at which ablation starts and one—at about 20–30% lower fluence—where the transmission breaks down. This behavior is attributed to a crystal area with a high density of defects. At the fluence where the transmission ceases,  $Ca^{(0)}$ , and to a much lesser extent,  $F^+$  are emitted ( $CaF^{(0)}$  was never observed at this lower threshold). Such emission represents true LID with the light absorption taking place at defect states in the bandgap. Therefore, it would be appropriate to call this effect ‘defect-assisted LID’. It must be realized that this observation is inherently connected with the low photon energy. For excimer laser irradiation defect absorption will be of less importance. Evidence is presented that the particle emission originates from structural defects like microcracks, generated by thermal stress. The emission of  $Ca^{(0)}$  at the transmission breakdown threshold has been shown to be delayed with a half-life of about 130 ms. The reason for this delay is still unknown.

The results discussed above represent only the beginning of a long-term project which will include the temperature dependence of particle emission, the influence of pulse- and wavelength on defect-assisted LID, as well as the controlled preparation of defect densities by electron bombardment. The incubation mechanism of  $CaF_2$  during multishot irradiation will have to be studied, and the question of surface metallization and possibly colloid formation must be followed up.

In the Introduction, the question was raised whether or not there are similarities in the LID and ESD mechanisms, as proposed by Itoh<sup>16,22</sup> and Bräunlich<sup>5,23</sup> and their collaborators for ultrapure crystals. On the basis of the data presented in this contribution for commercial ‘optical grade’ crystals we have to deny any similarity, at least for green light and nanosecond pulse lengths. The reason is the fundamentally different energy absorption mechanism. In ESD, electrons have sufficient energy to excite e-h pairs which relax, with a certain

efficiency, to separated color centers which can migrate to the surface and cause desorption. It is important to notice that electron bombardment does not lead to significant heating. Photons with energies much smaller than the band gap, on the other hand, can only be absorbed by defect states in the band gap. That causes predominantly local heating and thermal expansion rather than color center production. Within the nanosecond time interval the thermal load stays very localized and leads to microscopic damage, which is not to be confused with ablation. Particles then emerge from these microcracks at fluences much below the ablation threshold. Such model would be similar to what was proposed by Dickinson and collaborators.<sup>20,21,32</sup> In summary, we propose that the fundamental difference between ESD and LID with visible light is a consequence of the vastly different thermal load on the crystal in these two processes. It will be the task of future investigations to test this conjecture.

#### ACKNOWLEDGEMENT

This work is supported by Deutsche Forschungsgemeinschaft, Sfb 337. We thank Dr. T. A. Green for extensive and enlightening discussions.

#### REFERENCES

1. T. J. Chuang, *J. Vac. Sci. Technol.* **B3**, 1408 (1985); *Surf. Sci.* **178**, 763 (1986); and page 203 in Ref.11.
2. J. Heidberg, C. Langowski, G. Neubauer, M. Folman, *Surf. Sci.* **189/190**, 946 (1987).
3. F. Budde, A. V. Hamza, P. M. Fern, G. Ertl, D. Weide, P. Andresen, H.-J. Freund, *Phys. Rev. Lett.* **60**, 1518 (1988).
4. E. Matthias and T. A. Green, in 'Desorption Induced by Electronic Transitions, DIET IV', editors: G. Betz and P. Varga, Springer *Ser. Surf. Sci.* **19**, 112 (1990). (To correct a printing error, the reader should move the last four lines of page 114 and the first 12 lines of page 115 as a block to the top of page 114).
5. A. Schmid, P. Bräunlich, P. K. Rol, *Phys. Rev. Lett.* **35**, 1382 (1975).
6. L. L. Chase and L. K. Smith, in 'Laser Induced Damage in Optical Materials 1987', editors: H. E. Bennett *et al.*, *NIST Spec. Publ.* **756**, 165 (1988).
7. H. F. Arlinghaus, W. F. Calaway, D. M. Gruen, L. L. Chase, in 'Laser Induced Damage in Optical Materials 1988', editors: H. E. Bennett *et al.*, *NIST Spec. Publ.* **775**, 140 (1989).
8. W. J. Siekhaus, J. H. Kinney, D. Milam, L. L. Chase, *Appl. Phys.* **A39**, 163 (1986).
9. E. Matthias, H. B. Nielsen, J. Reif, A. Rosén, E. Westin, *J. Vac. Sci. Technol.* **B5**, 1415 (1987).
10. J. Reif, *Opt. Eng.* **28**, 1122 (1989).
11. A. Rosén, E. Westin, E. Matthias, H. B. Nielsen, J. Reif, *Phys. Scripta* **T23**, 184 (1988).
12. J. C. Miller and R. F. Haglund, Jr. (editors): 'Laser Ablation, Mechanisms and Applications', Lecture Notes in Physics **389**, Springer-Verlag Berlin Heidelberg 1991.
13. see also forthcoming Proceedings of 1992 Workshop on 'Desorption Induced by Electronic Transitions, DIET V', editor: A. R. Burns, to be published.
14. W. Hoheisel, M. Vollmer, F. Träger, page 77 in Ref. 12.
15. L. L. Chase, A. V. Hamza, H. W. H. Lee, page 193 in Ref.12.
16. N. Itoh, K. Hattori, Y. Nakai, J. Kanasaki, A. Okano, R. F. Haglund, page 213 in Ref.12.
17. M. A. Schildbach and A. V. Hamza, *Phys. Rev.* **B45**, 6197 (1992).
18. R. F. Haglund, Jr., M. Affatigato, J. H. Arps, K. Tang, A. Niehof, W. Heiland, *Nucl. Instr. Methods* **B65**, 206 (1992).
19. O. Kreitschitz, W. Husinsky, G. Betz, N. H. Tolk, to be published in Ref. 13 and in *Nucl. Instr. Methods B*.
20. R. L. Webb, L. C. Jensen, S. C. Langford, T. J. Dickinson, *J. Appl. Phys.*, **74**, 2323 (1993).
21. J. T. Dickinson, L. C. Jensen, R. L. Webb, M. L. Dawes, S. C. Langford, *J. Appl. Phys.* to be published.
22. K. Tanimura and N. Itoh, *Nucl. Instr. Methods* **B46**, 207 (1990).
23. S. C. Jones, P. Bräunlich, R. T. Casper, X.-A. Shen, P. Kelly, *Opt. Eng.* **28**, 1039 (1989).
24. E. Matthias and Z. L. Wu, *Appl. Phys.* **A56**, 95 (1993).
25. W. Hayes (editor): 'Crystals with the Fluorite Structure', Clarendon Press, Oxford 1974.
26. R. T. Williams, *Opt. Eng.* **28**, 1024 (1989).

27. A. S. Epifanov, *IEEE J. Quant. Electron.* QE-17, 2018 (1981).
28. J. Reif, H. Fallgren, H. B. Nielsen, E. Matthias, *Appl. Phys. Lett.* **49**, 930 (1986).
29. R. E. Walkup, Ph. Avouris, and A. P. Ghosh, *Phys. Rev.* **B36**, 4577 (1987).
30. R. E. Walkup and Ph. Avouris, *Phys. Rev. Lett.* **56**, 524 (1986).
31. T. A. Green and M. Riley, private communication.
32. J. T. Dickinson, M. J. Dresser, L. C. Jensen, in 'Desorption Induced by Electronic Transitions DIET II', editors: W. Brenig and D. Menzel, *Springer Ser. Surf. Sci.* **4**, 281(1985).